ISBN: 978-3-95450-227-1 ISSN: 2673-5490 doi:10.18429/JACoW-IPAC2022-THIXSP1

A NEW COMPACT 3 GeV LIGHT SOURCE IN JAPAN

N. Nishimori†, QST, Miyagi 980-8579, Japan

Abstract

A new 3 GeV light source with a circumference of 350 m and an MBA lattice is being constructed in north-eastern Japan. Aiming at stable and high-performance operations with an emittance of about 1 nm rad, various design and R&D activities are being performed: the four bend achromatic lattice using combined-function bend magnets; the compact RF system using a TM020 mode and in-cavity compact HOM absorbers; the in-vacuum off-axis injection scheme enabling stored beam oscillation-free injections with a small injection beam amplitude; the injector linac composed of a thermionic E-gun and C-band accelerators with a capability of extension to feed a future soft X-ray FEL driver, and so on. The installation of accelerator components is ongoing. The overall design of the light source, R&D results, and the latest construction status are presented.

INTRODUCTION

A new 3 GeV light source named NanoTerasu is under construction in Sendai, Japan [1]. The concepts of the light source are to build a highly brilliant compact soft X-ray (SX) source based on reliable and proven SPring-8 / SACLA accelerator technology, to be a complementary partner of SPring-8 to mainly cover the SX region, and to provide SX free-electron laser (SXFEL) in the future upgrade. The brilliance of the 3 GeV light source as a function of photon energy is represented by solid curves in Fig. 1 and those of SPring-8 by dotted curves. The main targets of NanoTerasu are EUV, SX and Tender X-ray regions where the brilliance is one to two orders of magnitudes higher than SPring-8. The target brilliance is 10^{21} photons/sec/mm^2/mrad^2/0.1% b.w. and coherent ratio of roughly 10 % for several keV photon energies. A multi-pole wiggler (MPW) serves as a hard X-ray source instead of a bending magnet. The above requirements can be satisfied with a beam energy of 3 GeV, stored current of 400 mA and horizontal beam emittance of 1 nm rad.

The initial portfolio of the first phase 10 beamlines under preparation was selected to meet the effective use of the low-emittance light source, needs of both academia and industry, and the complementary capability of other SR facilities in Japan. As shown in Fig. 2, there are two EUV/SX beamlines represented by orange, four SX by green, three Tender-X by purple and one HX by deep blue.

Polarization dependence in soft X-ray spectroscopy allows the investigation of electronic states in materials. In EUV/SX region, polarization is controlled by insertion devices such as APPLE-II because of the lack of polarizers. Resonant inelastic X-ray scattering will be used to probe charge, magnetic and orbital degrees of freedom on selected atomic species of various solid, liquid, and gas targets under various environments. Photoemission spectroscopy beamlines are used to measure the electronic structure of the materials to analyze the properties of catalysts, battery electrodes, and so on under the operating environment. X-ray magnetic circular dichroism beamline employs a four-segment APPLE-II crossed undulator for research of magnetic materials and devices [2], because fast and versatile control of polarization is feasible by phase shifters, and higher polarization up to 0.6 is obtained with four segments [3]. In addition, the generation of higher harmonic circular polarization is feasible by using high flux higher harmonic linear polarized light from APPLE-II.

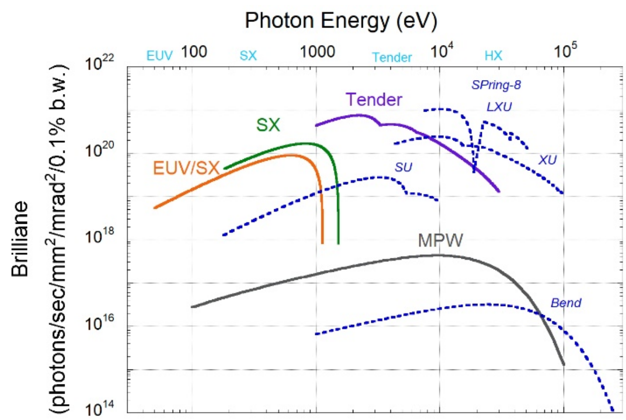

Figure 1: Brilliance as a function of photon energy.

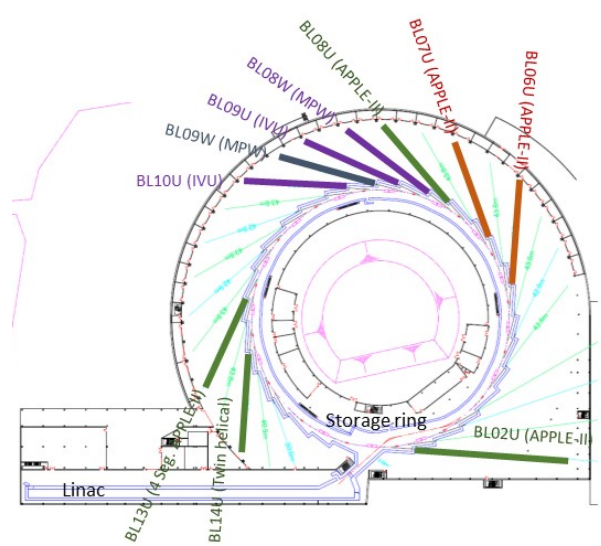

Figure 2: Layout of the 3GeV light source NanoTerasu.

In vacuum undulators (IVUs) and MPWs will be used as tender and hard X light sources above 2 keV. Hard X-ray photoemission spectroscopy and X-ray absorption fine structure (XAFS) will be used to investigate bulk

†nishimori.nobuyuki@qst.go.jp

ISBN: 978-3-95450-227-1 ISSN: 2673-5490 doi:10.18429/JACoW-IPAC2022-THIXSP1

electronic and geometric structures under operando conditions. Coherent diffraction imaging and ptychography will be used to visualize the spatial distribution of electron density and lattice distortion of a sample at mesoscale.

High intensity X-rays with a continuous spectrum from MPW are used for small-angle X-ray scattering and XAFS to obtain information on the chemical state and structure as well as X-ray multiscale structure analysis.

ACCELERATOR SYSTEM

The accelerator complex of the new 3 GeV facility is composed of a compact storage ring with a circumference of 350 m and a compact 110 m injector linac. The design details are described in Refs. [1,4]. A 4-bend achromat (4BA) lattice with 16 cells is chosen for the ring to achieve the low emittance. The lattice functions of NanoTerasu are shown in Figure 3. The red and blue curves are horizontal and vertical β-functions and the green curve is dispersion function. Four combined-function bends, 10 quadrupoles and 10 sextupoles are employed in the 4BA lattice. Eight quadrupoles are used to horizontally focus the beam at bends and 4 combined-function bends and two quadrupoles are used to vertically focus the beam. Each cell serves a long straight of 5.4 m for an undulator and a short straight of 1.6 m for an MPW except for the cells assigned for beam injection, RF cavities, and beam diagnostic instruments.

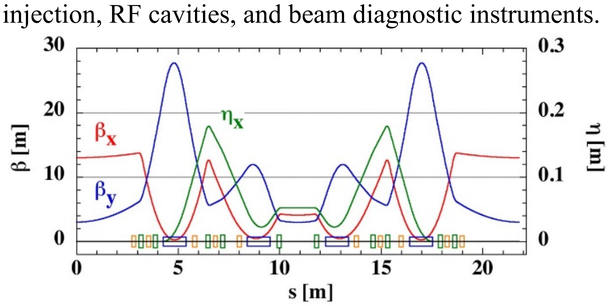

Figure 3: Lattice functions of NanoTerasu.

Magnet

Our concept is to build a system with a small number of magnet types and power supplies which results in an advantage for mass production and low failure probability of power supply, that is for low cost and easy maintenance. Figure 4 shows a lineup of magnets in one cell. The combined-function bends are all the same. Quadrupoles are two types, Q1 and *Q3* which is designed to avoid interference with X-ray beamlines. Sextupoles are also two types, S1 and *S4*. Therefore, only five types are used as main magnets.

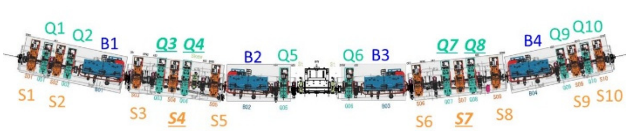

Figure 4: Magnet system in each cell.

There are 11 sets of family magnets: 1 bend, 5 quadrupoles, and 5 sextupoles. Each family of magnets is powered in series by a common power supply and 11 power supplies are prepared. Our concept requires a small field deviation between mass-produced magnets.

The number and parameters of all the type of SR magnets are listed in Table 1. The core of multipole magnets is laminated silicon steel with a thickness of 0.5 mm. The bore diameter is 34 mm for quadrupoles and 40 mm for sextupoles. The pole gap is 12.4 mm to obtain a high gradient. The effective length is 200 mm. The requirement of field deviation is within ±0.4%. An auxiliary power supply is connected to an individual quad for independent adjustment of the magnetic field. The sextupoles are equipped with auxiliary coils working as steering magnets as well as fine-tuning of sextupole. The core type of combined-function bend is massive steel. The cross-section is a truncated hyperbolic curve to incorporate defocusing quadrupole and to decrease emittance. The pole gap is 28 mm along the beam trajectory. The effective magnetic length is 1130 mm along the arc orbit. The requirements for dipole and quadrupole field deviations are less than 0.2 % and 0.4 %, respectively.

All the multipole magnetic fields were measured with a single stretched wire system. The field deviations from the average for a family of 32 quadrupoles or 32 sextupoles are well within 0.4 % specification. The magnetic field of combined-function bend is measured with a 3D Hall-probe system. The bending field deviations from the average are within 0.2% and those for quadrupole are within 0.4% satisfying requirements.

Table 1: The Number and Main Parameters of SR Magnets

Parameter	Quadrupole		Sextupole		Combined-function bend
Type	Q1	*Q3*	S1	*S4*	B
Number/ring	96	64	128	32	64
Core Type	Laminated steel				Massive steel
Bore diameter	34 mm		40 mm		
Pole gap	12.4 mm				28 mm at center
Effective length	200 mm				1130 mm
Field deviation	±0.4 %				±0.2 % (B) ±0.4 % (Q)

Vacuum

The vacuum system is designed to allow gas scattering lifetime of more than 20 hours at a stored electron beam current of 400 mA, requiring the average vacuum pressure of 1×10^{-7} Pa equivalent to CO. A thin stainless steel (316) chamber with 2 mm thickness and copper plating inside is employed to meet the short magnet gap of our 4BA lattice and to reduce resistive wall impedance. The shortest gap of multipole magnets and the height of vacuum chambers are 12.4 mm and 10 mm, respectively, and the clearance between magnet and chamber is 1.2 mm, as shown in Figure 5.

ISBN: 978-3-95450-227-1 ISSN: 2673-5490 doi:10.18429/JACoW-IPAC2022-THIXSP1

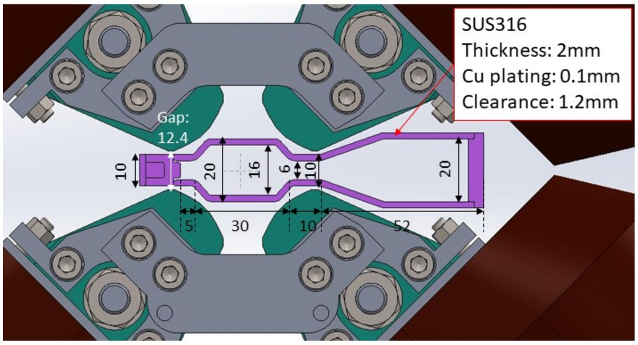

Figure 5: Cross section of a vacuum chamber in a quadrupole magnet.

Discretely arranged 10 photon absorbers, 2 crotch absorbers, and 4 supplemental absorbers together with vacuum pumps nearby are used to absorb SR from bending magnets and to localize and evacuate photon stimulated desorption (PSD) gas effectively. The absorbers are placed at 17 or 29 mm apart from the electron beam trajectory. The vacuum chambers are therefore horizontally compact as well as magnets. Only 4 types of photon absorbers are designed and manufactured for low cost and easy maintenance. They are one for absorbers (AB), two for crotch absorbers for undulator and MPW, and one for supplemental absorbers (SAB). Absorbers and crotch absorbers are made of GLIDCOP and SABs are made of oxygen free copper. The maximum SR peak power density on absorbers is estimated to be about 200 W/mm^2. The vacuum pressure distribution in a unit cell at 400 mA operation after 1500 Ah conditioning is calculated and the average pressure of CO is estimated to be 6×10^{-8} Pa corresponding to the gas scattering lifetime of about 22 hours.

A stored electron beam needs to be dumped in a controlled way during beam abort, which is initiated by RF power off. The beam loses energy turn-by-turn and eventually hits vacuum chambers. To avoid vacuum incidents, an elaborately prepared electron beam absorber is installed in every cell for the high-density beam to be spread out before striking chambers.

A vertical beam shaker with a frequency close to vertical betatron tune is employed to decrease the beam vertical density by 300 [5-7]. Graphite beam absorbers, the surface of which sticks out by 5 mm from the inside of the vacuum chambers, are installed where dispersion function is maximum and the ring tunnel wall is most distant from the chambers. That is the chamber near 8-th quadrupole in Figure 4.

RF

The radiation loss per turn in NanoTerasu is estimated to be 1.26 MeV where 0.62 MeV is lost in bends and the rest is lost in insertion devices. An RF power of 500 kW is thus required for compensating the radiation loss of a 400 mA beam. To make the beam lifetime longer than 10 hours, an RF accelerating voltage of 3.6 MV is required. We install 4 sets of 509 MHz acceleration cavities on one of 5.4 m long straight sections. A new type of compact TM020-mode normal conducting cavity has been developed to accommodate the space limitation [8]. The TM020 cavity has nodes of the magnetic field at the fundamental mode inside the cavity. We prepared slots along the nodes and installed ferrite to damp higher-order modes (HOMs) entering the slots, because those HOMs excited in the cavity cause coupled-bunch instability. HOMs are dissipated on the ferrite dampers while the fundamental mode is not damped.

The shunt impedance of the new cavity is estimated to be 6.8 MΩ and RF power of 120 kW per cavity is required for 0.9 MV acceleration, which corresponds to 3.6 MV acceleration and 480 kW RF power per four total cavities. The klystron RF power of 1 MW is thus required for 400 mA stored beam operation.

We performed high power test of a TM020-mode cavity and 120 kW power was successfully fed into the cavity equipped with 12 HOM absorbers with a vacuum pressure of 1.5×10^{-6} Pa.

Ring Beam Injection

An in-vacuum windowless off-axis beam injection system from the ring inside is employed for stable and transparent beam injection together with the capability of top-up operation [9]. The injection system consists of a windowless beam transport, two DC septum magnets, an in-vacuum pulse septum magnet, and a pair of twin kickers having identical magnet characteristics. The system allows a small oscillation amplitude of injected electron beam of around 7.5 mm and stored beam oscillation amplitude less than 10 µm satisfying transparent beam injection during the top-up operation. A differential pump-system upstream DC septa separates the ring vacuum from beam transport.

The bumped beam trajectory is 7.5 mm apart from the stored beam and the injected beam is located 7.5 mm from the bumped beam. The septum wall of thickness 1 mm is located 2.5 mm from the bumped beam and 4 mm from the injected beam. The length and kick angle of each kicker are 300 mm and 6 mrad, respectively, those of pulse septum are 500 mm and 70 mrad, and those of DC septum are 400 mm and 48 mrad.

Twin kickers are driven by a single solid state pulser to generate identical kicker magnetic pulses [10]. The pulser consists of a charging circuit up to 55 kV, a main capacitor of 65 nF and a fast IGBT switch to provide peak current of 1.6 kA and half-sine pulse width of 3 µs. The fluctuation of the charging voltage is measured to be 0.01 %, indicating good reproducibility. The magnetic property of the kicker, such as inductance, should be identical with another kicker [11]. We measured the inductance as a function of frequency and the difference is found to be less than 0.2 % up to 1 MHz, which can be corrected with a variable inductor of the pulser. The difference between measured temporal profiles of magnetic fields of twin kickers is demonstrated to be $\pm$ 0.1 % satisfying specification. Ceramic vacuum chambers with uniform titanium (Ti) coating with 3µm thickness are used. The magnetic field is attenuated by 3 % due to the eddy current in the coating

ISBN: 978-3-95450-227-1 ISSN: 2673-5490 doi:10.18429/JACoW-IPAC2022-THIXSP1

and the attenuation will be compensated by increasing the power supply output. Ceramic chambers with patterned inner Ti-coating to reduce the eddy current is under development.

The in-vacuum pulse septum has a thin septum wall with a thickness of 0.5 mm for stored and injected beams to get closer for small injected-beam oscillation amplitude. The magnet gap is 2 mm which is narrow enough to provide 1.4 T pulsed magnetic field uniformly along the horizontal axis over 4 mm. The stray field integral outside of the septum goes down to 10^{-5} Tm or less by using a permalloy magnetic shield. The vacuum pressure is measured to be less than 3×10^{-8} Pa. We measured the pulsed magnetic field as a function of horizontal position with a thin search coil. The field is almost flat within ±0.2 % from 2 mm to 5 mm from the septum wall, where the injected beam passes.

Injector Linac

A compact full-energy injector capable of driving SXFEL in the future is employed. A high gradient C-band disk-loaded traveling-wave-type accelerating cavity with a 42 MV/m gradient [12], which is modified from the original choke mode type cavity developed at SACLA [13], is employed to achieve 3 GeV full energy acceleration. Twenty units of the C-band accelerator system are installed in the linac tunnel. The unit consists of two C-band 2 m-long-cavities fed by a 50 MW pulsed klystron. Each klystron is driven with 350 kV, 310 A pulse power supplied by a modulator, and 300 W RF input supplied by a driver amplifier. The RF output power from the klystron is compressed by an RF pulse compressor (SLED) by a factor of 4 to supply 80 MW peak power to each accelerator cavity.

A newly developed 500 kV electron gun consisting of a 50 kV DC gun equipped with a commercially available gridded thermionic cathode (CPI Y845) and a 238 MHz RF accelerator cavity is employed [14,15]. While the emittance is believed to be deteriorated by a grid effect, it is demonstrated that a low emittance beam can be generated in a transparent grid scheme where the grid potential is matched to the potential formed by cathode anode voltage as if no grid exists. We measured the beam current, bunch charge and normalized emittance as a function of grid voltage and found the emittance is minimum when the transparent grid scheme is satisfied [16]. The measured minimum normalized emittance for a core part which represents 60 % of a 1 nC electron bunch is 1.5 μmrad making the transparent-gridded thermionic gun an electron source for an SXFEL.

SCHEDULE AND STATUS

Schedule

Most of the components were designed by 2019, and the production phase started in 2020. Some of the magnets were already installed in the storage ring tunnel. The beam commissioning will start in 2023 and user operation is scheduled in 2024. The linac components such as C-band accelerators were already produced and some of them were installed in the linac tunnel. Many components such as SR magnets, vacuum chambers, RF cavities, and an electron gun are first tested at SPring-8 after production and transported to the 3 GeV site.

Status

All the magnets for the storage ring are assembled on the girders in the magnet production factory. The final precise alignment for each girder is performed in the on-site alignment area at the experimental hall, as shown in Figure 6. A vibrating wire method (VWM) technique is employed for the alignment of on-girder multipole magnets with an accuracy of 50 μm for all the girders [17] and a laser tracker is used for alignment between girders and bends with an accuracy of 90 μm.

We prepared 4 temperature-controlled booths with the stability of <0.1 °C at the experimental hall where 4 VWM alignments are performed at the same time as well as a stock area where 24 girders corresponding to 4 cells can be stocked is also prepared at the experimental hall.

We perform VWM alignments for 6 girders corresponding to 1 cell in a week and install them to the storage ring tunnel and transport new 6 girders from the production factory. The girders are transported to the tunnel through the temporary opening of the tunnel and placed on the two supporting pillars. Those pillars are placed on a specially prepared flat floor surface made of epoxy resin by self-leveling technique. The tilt of the surface is less than 50 μm/m. No shim plate is necessary between floor and pillar. The vibration transfer from the floor to the girders is greatly suppressed by the surface flatness. The radiation hardness of the epoxy resin has been experimentally verified by Cobalt 60 source up to 1 MGy [18]. It takes 16 weeks for 16 cells alignment and installation in the ring tunnel.

We fabricated a vacuum chamber prototype and assembled it to the magnet system to check interference with magnets and other components at SPring-8. A leak test and 150°C baking for 20 hours followed by NEG activation were performed for the prototype and ultimate vacuum pressure less than 10^{-8} Pa satisfying the requirement was obtained. No interference was found during the assembly of the prototype. The mass-production of vacuum chambers is on schedule and installation to the accelerator tunnel begins this June.

ISBN: 978-3-95450-227-1 ISSN: 2673-5490 doi:10.18429/JACoW-IPAC2022-THIXSP1

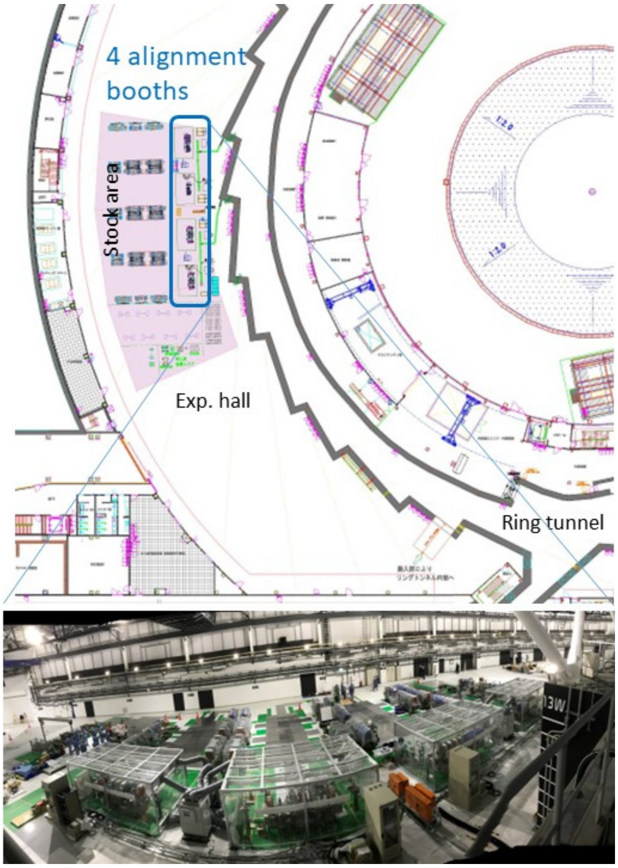

Figure 6: On-site alignment area for SR magnets at the experimental hall.

SUMMARY

Our concept of a new compact 3 GeV light source is presented. Hardware production and installation are in progress. We will finish the installation phase and start beam commissioning by the middle of 2023. User operation is scheduled to start in FY2024.

ACKNOWLEDGMENTS

We would like to thank all the members of the 3 GeV accelerator working group at QST, JASRI and RIKEN for their contributions to the 3 GeV compact light source project.

REFERENCES

[1] N. Nishimori, T. Watanabe, and H. Tanaka, "A Highly Brilliant compact 3 GeV Light Source Project in Japan", in *Proc*. IPAC'19, Melbourne, Australia, May 2019, pp. 1478-1481. doi:10.18429/JACoW-IPAC2019-TUPGW035

[2] I. Matsuda *et al*., "Segmented Undulator for Extensive Polarization Controls in ≤1 nm-rad Emittance Rings", *e-J. Surf. Sci. Nanotechnol.* 17, 41-48 (2019). doi:10.1380/ejssnt.2019.41

[3] J. Miyawaki *et al*., AAPPS Bulletin 31, 25 (2021).

[4] QST, "Accelerator design report for 3-GeV Next-Generation Synchrotron Radiation Facility", Sep. 2020, https://www.qst.go.jp/uploaded/attachment/18596.pdf

[5] T. Hiraiwa *et al*., "Interpretation of Particle Motion in a Circular Accelerator as Diffraction of Light", presented at IPAC'22, Bangkok, Thailand, Jun. 2022, paper WEIZSP1, this conference.

[6] T. Hiraiwa, K. Soutome, and H. Tanaka, "Forced harmonic oscillator interpreted as diffraction of light", *Phys. Rev. E* 102, 032211 (2020). doi: 10.1103/PhysRevE.102.032211

[7] T. Hiraiwa, K. Soutome, and H. Tanaka, "Formulation of electron motion in a storage ring with a betatron tune varying with time and a dipole shaker working at a constant frequency", *Phys. Rev. Accel. Beams* 24, 114001 (2021). doi: 0.1103/PhysRevAccelBeams.24.114001

[8] H. Ego, "Design of a HOM-damped RF Cavity for the Spring-8-II Storage Ring", in *Proc.* of the 11th Annual Meeting of Particle Accelerator Society of Japan, pp. 237-241, Aomori, Japan, Aug. 2014, paper MOOL14 (in Japanese).

[9] S. Takano *et al*., "Renovation of off-axis beam injection scheme for next-generation photon source", in *Proc*. IPAC'19, Melbourne, Australia, May 2019, pp. 2318-2321. doi:10.18429/JACoW-IPAC2019-WEPMP009

[10] T. Inagaki *et al*., "Development of a solid-state pulse generator driving kicker magnets for a novel injection system of a low emittance storage ring", in *Proc*. of IPAC'18, Vancouver, Canada, Apr.-May 2018, pp. 1804-1807. doi:10.18429/JACoW-IPAC2018-WEYGBF4

[11] K. Fukami *et al*., "Iron lamination and interlaminar insulation for high-frequency pulsed magnets", *Rev. Sci. Instrum*. 93, 023301 (2022). doi:10.1063/5.0074226

[12] T. Sakurai *et al*., "C-band disk-loaded-type accelerating structure for a high acceleration gradient and high-repetition-rate operation", *Phys. Rev. Accel. Beams* 20, 042003 (2017). doi: 10.1103/PhysRevAccelBeams.20.042003

[13] T. Inagaki *et al*., "High-gradient C-band linac for a compact x-ray free-electron laser facility", *Phys. Rev. ST Accel. Beams* 17, 080702 (2014). doi: 10.1103/PhysRevSTAB.17.080702

[14] T. Asaka *et al*., "Low-Emittance Compact RF Electron gun with a Gridded Thermionic Cathode", presented at IPAC'22, Bangkok, Thailand, Jun. 2022, paper FRIXSP1, this conference.

[15] T. Asaka, et al., "Low-emittance radio-frequency electron gun using a gridded thermionic cathode", *Phys. Rev. Accel. Beams* 23, 063401 (2020). doi: 10.1103/PhysRevAccelBeams.23.063401

[16] T. Asaka, et al., "Transparent-grid scheme for generating cathode-emittance-dominated beams in a gridded thermionic gun", *Jpn. J. Appl. Phys.* 60, 017001 (2021). doi: 10.35848/1347-4065/abd0c9

[17] K. Fukami *et al*., "Performance verification of a precise vibrating-wire magnet alignment technique for next-generation light sources", *Rev. Sci. Instrum*. 90, 054703 (2019). doi:10.1063/1.5086505

[18] H. Kimura, "A Radiation test of epoxy self-keveking materials for high precision flat floor surface", in *Proc*. of the 11th Annual Meeting of Particle Accelerator Society of Japan, pp. 908−911, Aomori, Japan, Aug. 2014, paper SAP131 (in Japanese).